

Dimensions and the profile of surface nanobubbles: Tip-nanobubble interactions and nanobubble deformation in Atomic Force Microscopy

*Wiktoria Walczyk and Holger Schönherr**

Physical Chemistry I, Department of Chemistry and Biology, University of Siegen, Adolf-
Reichwein-Str. 2, 57076 Siegen, Germany

Corresponding Author

* schoenherr@chemie.uni-siegen.de

Supporting Information

EXPERIMENTAL

Sample preparation: In all experiments freshly cleaved highly oriented pyrolytic graphite (HOPG) (grade ZYH, VeecoO, Santa Barbara, CA) with a water contact angle of $63 \pm 2^\circ$ was used. The static contact angle was measured with the sessile drop method with an OCA 15plus instrument (Data Physics Instruments GmbH, Filderstadt, Germany) using Milli-Q water obtained from a Millipore Direct Q 8 system (Millipore, Schwalbach, Germany) with resistivity of 18.0 M Ω /cm and surface tension of 0.072 N/m (determined by a Wilhelmi plate method). Nanobubbles were measured in Argon saturated Milli-Q water. First, 20 mL of Milli-Q in a clean round-bottom flask with a Teflon inlet were degassed at a pressure of 80 mbar for 30 min at 20°C by using a diaphragm vacuum pump (Type MZ 2C, Vacuubrand, Germany), while it was sonicated continuously in a water bath sonicator (Brandelin Sonorex, Rk 100 H). Next, the flask with water was closed, removed from the ultrasonic bath, and was put under an Ar stream (no filter used) for 45 min.

Atomic Force Microscopy: The AFM measurements were carried out on a MultiMode IIIa AFM instrument (Bruker/Veeco/Digital Instruments, Santa Barbara, CA) with a vertical engage E-scanner and NanoScope version 3.10 software (Bruker / Veeco, Santa Barbara, CA). V-shaped MLTC Si₃N₄ cantilevers (Bruker AXS, Camarillo, CA) with the following spring constants were used: $k_{cant} = 0.1 \pm 0.01$ N/m and $k_{cant} = 0.7 \pm 0.07$ N/m. The cantilevers' spring constants were calibrated on an Asylum Research MFP-3D Bio (Asylum Research, Santa Barbara, California). The cantilevers were cleaned prior to the measurements for 60 s by oxygen plasma (Plasma Prep-II, SPI Supplies, West Chester, USA). In order to minimize the contamination of the tip, the cantilevers were inserted with minimal delay in the liquid cell and directly immersed in water.

In all experiments, a closed liquid cell configuration was used. First, the liquid cell, the O-ring (fluorosilicone rubber) and the inlet and outlet tubes (silicone) were rinsed with Milli-Q water and with ethanol (99.9 %, Merck KGaA, Darmstadt, Germany) and dried in a stream of nitrogen. Next, the liquid cell was assembled and the cantilever was inserted. Subsequently, a 1 mL sterile syringe (Braun, Injekt-F 0.01-1ml/luer Solo) was filled with the Ar saturated water and connected to the inlet tube. No needle was used for this procedure in order to avoid the possible contamination by the lubricant. Immediately, the water was injected in the liquid cell until the cantilever was immersed and the O-ring was filled. Then the liquid cell was placed on the sample, the O-ring was brought in contact with the sample, 0.6 mL of water was passed through the liquid cell and after that the inlet and outlet were closed. We stress that *no* liquid exchange procedure was performed and the HOPG surface did not have contact with ethanol at any stage of the experiment. Also, the lubricant free syringe used was cleaned by Milli-Q water before use. Before the start of the AFM measurement, the system was left for 30 min to equilibrate. The nanobubbles were scanned first in TM AFM and subsequently in FV mode without changing the cantilever and the tip or replacing the liquid.

Tapping mode (TM AFM): The drive frequency used for imaging in TM AFM was 9.2 kHz for the cantilever with $k_{cant} = 0.1 \pm 0.01$ N/m, and 29.6 kHz for the cantilever with $k_{cant} = 0.7 \pm 0.07$ N/m. The free amplitude of the cantilever oscillations (in Volts) was calculated from amplitude-displacement curves recorded before and after recording of the image, as an average of 50 points. Next, it was converted into free amplitude in nanometers using the appropriate value of the deflection sensitivity. The amplitude setpoint ratio (ratio of the setpoint amplitude value set during the measurements and free amplitude calculated from the corresponding amplitude-distance curve) was calculated as the mean value of two setpoint ratios determined using amplitude-distance curves recorded before and after scanning a TM height image. The values of free amplitudes and setpoint ratios in TM measurements of

nanobubbles in our experiments were 13 nm and 90 % for the experiment done with the cantilever with $k_{cant} = 0.1 \pm 0.01$ N/m, and 16 nm and 90 % for the experiment done with the cantilever with $k_{cant} = 0.7 \pm 0.07$ N/m. Raw TM height images were processed using a 1st order plane fit and a 0th order flattening (any nanobubble was excluded). No tip size correction was applied. The bubble size was measured using the spherical cap fitting.

Force Volume mode (FV AFM): In this mode the tip was lowered and retracted at each point of the selected area of the sample and the interaction forces during approach and retraction were measured. The resolution of the imaging was limited to 32×32 pixels². The cantilever oscillation was switched off during data acquisition in FV mode. Ramp sizes and trigger thresholds were set to 223 nm and 30 nm in the experiment done with the cantilever with $k_{cant} = 0.1 \pm 0.01$ N/m, and to 100 nm and 60 nm in the experiment done with the cantilever with $k_{cant} = 0.7 \pm 0.07$ N/m. The velocity of tip approach was set to 446 nm/s and 1.02 $\mu\text{m/s}$, respectively. The force curve resolution was set to 512 points per single approach-retraction cycle. Raw deflection-distance curves were transformed into deflection-separation curves. The vertical position of the tip above the *substrate* is represented in the plots by the tip-sample separation distance (zero separation indicates that the tip is in contact with the substrate). The deflection was recalculated into force by multiplying the measured deflection value with the corresponding cantilever stiffness.

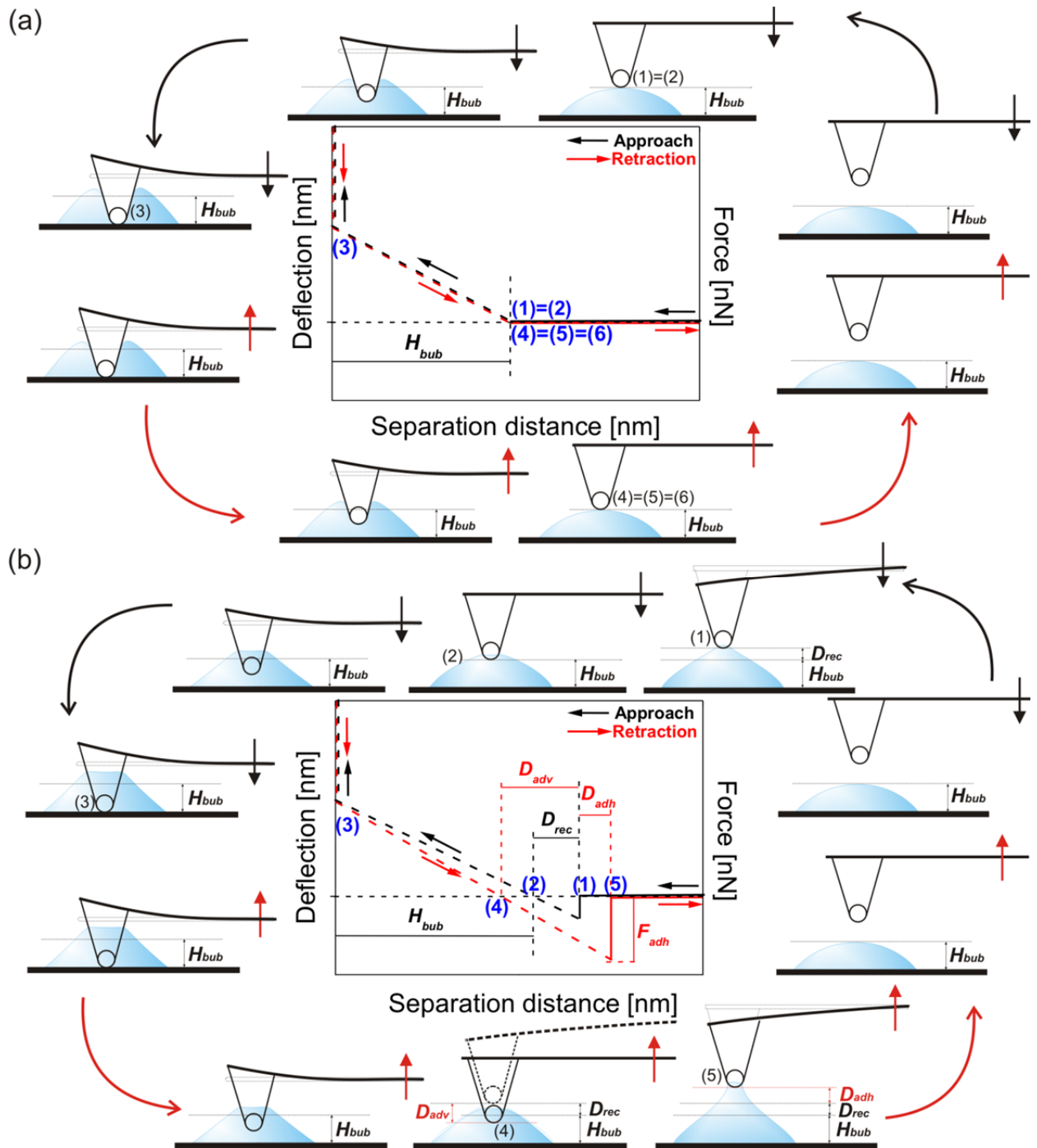


Figure S-1. Typical approach and retraction force-distance curves acquired on a nanobubble (a) with a hydrophilic AFM tip, (b) with a hydrophobic AFM tip. The parameters are described in the article. The schemes surrounding the plots show in a simplified way the position of the tip, the bending of the cantilever and the possible deformation of the bubble-water interface at different stages of a single approach-retraction force curve cycle (drawing not to scale). Importantly, in the experiment, the actual shape of the bubble might change differently during the interaction with a real AFM tip.

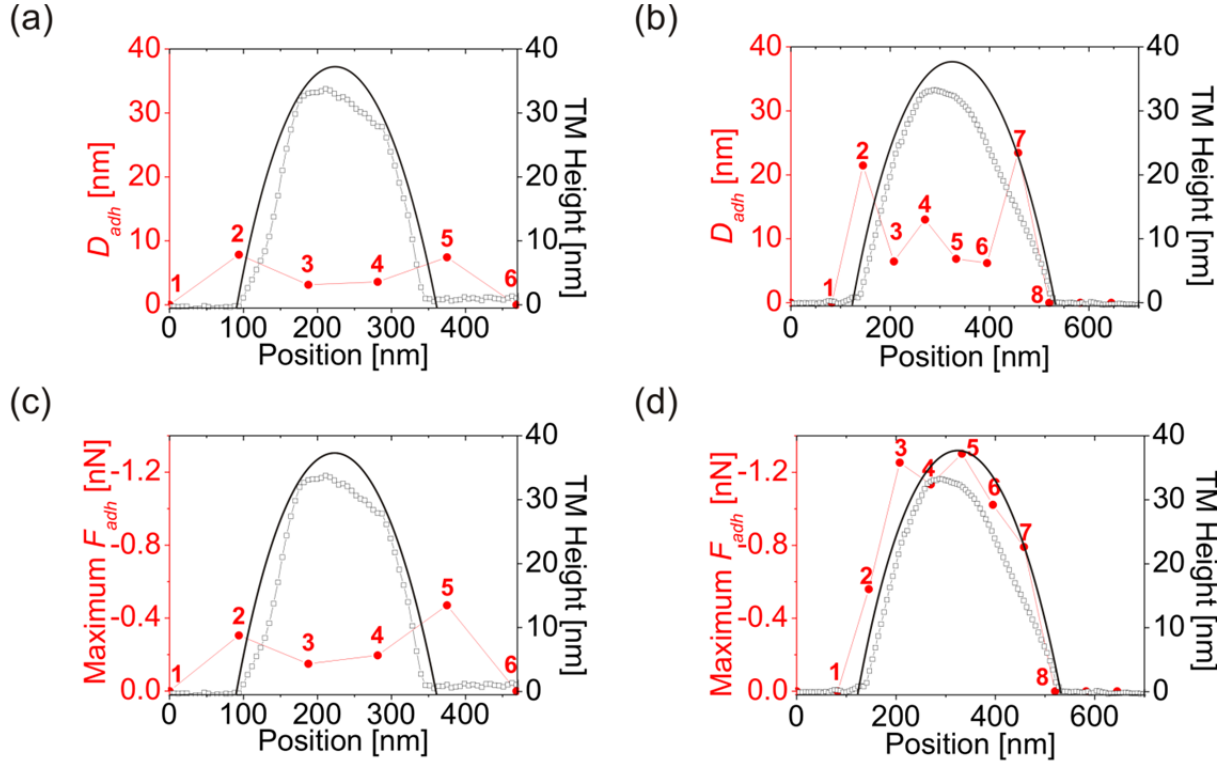


Figure S-2. (a) D_{adh} measured for the nanobubble scanned with a hydrophilic tip, (b) D_{adh} measured for the nanobubble scanned with a hydrophobic tip, (c) F_{adh} measured for the nanobubble scanned with a hydrophilic tip, (d) F_{adh} measured for the nanobubble scanned with a hydrophobic tip. In each cross-sectional plot, the values are plotted as a function of the horizontal position of the AFM tip along the scan line. The data measured from the force curves (solid red circles) are compared with the apparent (open black squares) and estimated (solid line) bubble profiles from TM AFM height images.

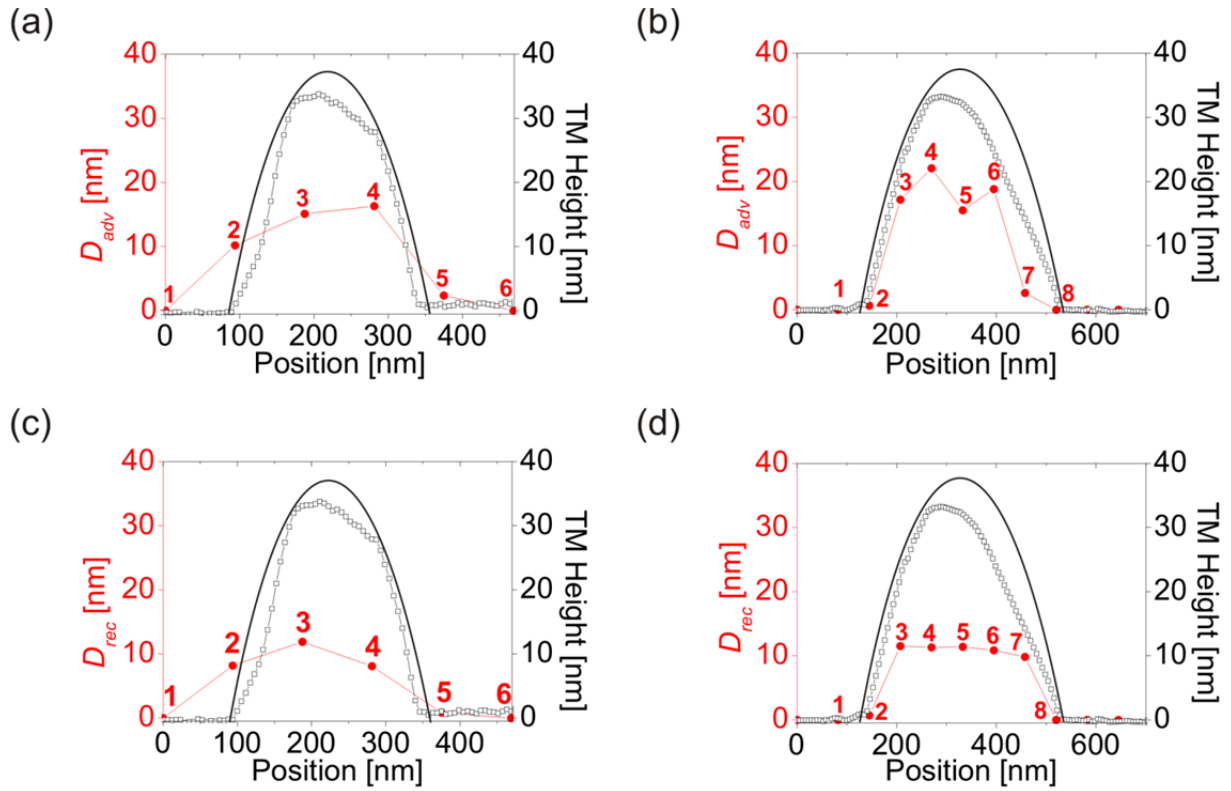


Figure S-3. (a) D_{adv} measured for the nanobubble scanned with a hydrophilic tip, (b) D_{rec} measured for the nanobubble scanned with a hydrophobic tip, (c) D_{adv} measured for the nanobubble scanned with a hydrophilic tip, (d) D_{rec} measured for the nanobubble scanned with a hydrophobic tip. In each cross-sectional plot the values are plotted as a function of the horizontal position of the AFM tip along the scan line. The data measured from the force curves (solid red circles) are compared with the apparent (open black squares) and estimated (solid line) bubble profiles from TM AFM height images.

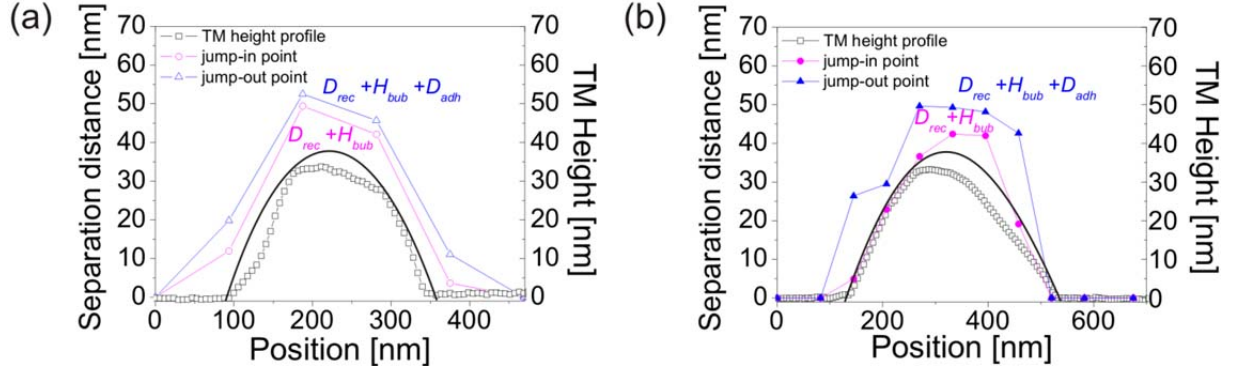


Figure S-4. The position of the jump-in and jump-out points in the force-distance curves marking the onset and the end of the tip-nanobubble interaction (contact), respectively, measured for the bubble scanned with (a) a hydrophilic tip, (b) a hydrophobic tip. The values are plotted as a function of the horizontal position of the tip along the scan line.

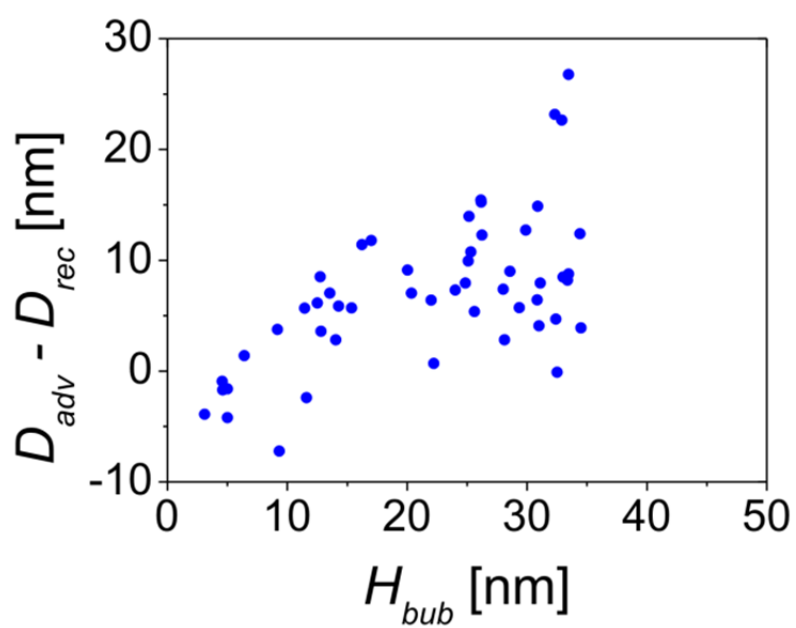


Figure S-5. Difference between the distances D_{adv} and D_{rec} as a function of the unperturbed local bubble height H_{bub} , measured from the force-distance curves acquired on the nanobubble with a hydrophobic tip.

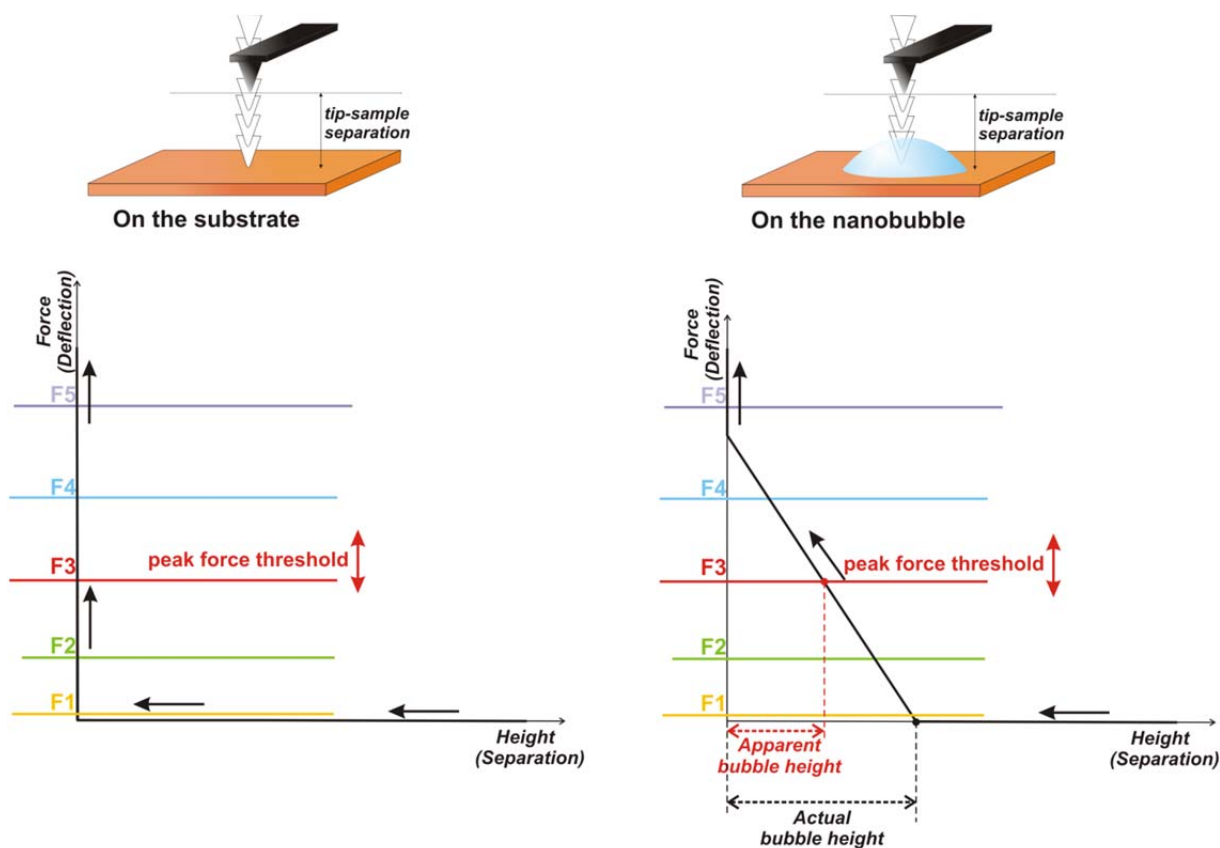


Figure S-6. Schematic shapes of AFM force-distance curves acquired on a hard substrate (left) and on a soft nanobubble (right). The horizontal lines define the exemplary setpoint values (denoted peak force thresholds) set by the peak force. The separation distance of the zero-deflection crossing point in the force curve on the right denotes the actual bubble height. The separation distance of the crossing point of the slope in the force curve with the line representing the force level indicates the apparent bubble height, as would be measured in an AFM height image scanned with this particular peak force.

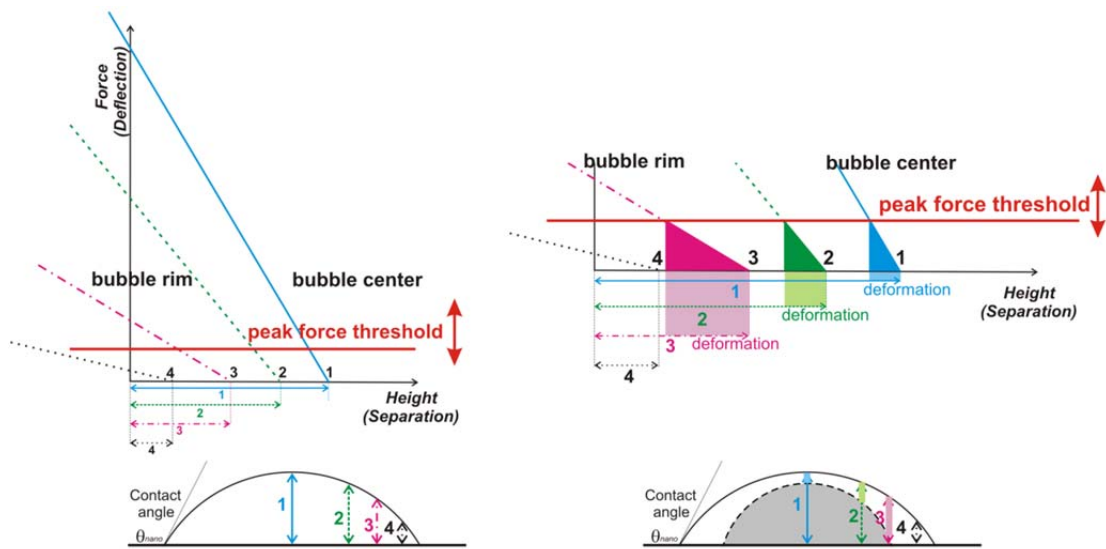


Figure S-7. The effect of varying steepness of the slopes of the force-distance curves on the measurement of the apparent nanobubble height. For a fixed peak force threshold, the apparent bubble height will be underestimated more and the bubble will be deformed to a larger extent near the bubble rim (less steep slopes) than near the bubble center (steeper slopes). A non-uniform underestimation of the actual bubble height will lead to a more protruding bubble shape with an underestimated width of the base and a smaller apparent contact angle (water side).